Climate change drives uncertain global shifts in potential distribution and seasonal risk of *Aedes*-transmitted viruses

Sadie J. Ryan[1,2,3*†], Colin J. Carlson[4*], Erin A. Mordecai[5], Leah R. Johnson[6]

Affiliations:

[1]Department of Geography, University of Florida, Gainesville, Florida, United States of America

[2] Emerging Pathogens Institute, University of Florida, Gainesville, Florida, United States of America

[3] School of Life Sciences, University of KwaZulu-Natal, Durban, South Africa

[4] Department of Environmental Science, Policy, and Management, University of California, Berkeley, 130 Mulford Hall, Berkeley, California, United States of America

[5] Department of Biology, Stanford University, 371 Serra Mall, Stanford, California, United States of America

[6] Department of Statistics, Virginia Polytechnic and State University, 250 Drillfield Drive, Blacksburg, Virginia, United States of America

*These authors share lead author status and contributed equally.

[†] **Corresponding author:** sjryan@ufl.edu

Climate change is likely to have a profound effect on the global distribution and burden of infectious diseases[1–3]. Current knowledge suggests that mosquito-borne diseases could expand dramatically in response to climate change[4,5]. However, the physiological and epidemiological relationships between mosquito vectors and the environment are complex and often non-linear, and experimental work has showed an idiosyncratic relationship between warming temperatures and disease transmission[6,7]. Accurately forecasting the potential impacts of climate change on *Aedes*-borne viruses—especially dengue, chikungunya, and Zika—thus becomes a key problem for public health preparedness[4,8,9]. We apply an empirically parameterized Bayesian model of *Aedes* transmission of these viruses as a function of temperature[6] to predict cumulative monthly global transmission risk in current climates, and compare against projected risk in 2050 and 2070 based on general circulation models (GCMs). Our results show that shifting suitability will track optimal temperatures for transmission (26-29 °C), potentially leading to poleward shifts. Furthermore, especially for *Ae. albopictus*, extreme temperatures are likely to limit transmission risk in current zones of endemicity, especially the tropics. The patterns of impact of changing minimum and maximum predicted temperatures lead to idiosyncratic outcomes for people at risk in the future. Validating these results with observed epidemic dynamics in upcoming decades will be paramount if global public health infrastructure is expected to keep pace with expanding vector-borne disease.

The intensification and expansion of vector-borne disease is likely to be one of the most significant threats posed by climate change to human health[2,10]. Mosquito vectors are of special concern, due to the global morbidity and mortality from diseases like malaria and dengue fever, as well as the prominent public health crises caused by (or feared from) several recently-emergent viral diseases like West Nile, chikungunya, and Zika. The relationship between climate change and mosquito-borne disease is perhaps best studied, in both experimental and modeling work, for malaria and its associated *Anopheles* vectors. While climate change could exacerbate the burden of malaria at local scales, more recent evidence challenges the “warmer-sicker world” expectation[11]. The optimal temperature for malaria transmission

has recently been demonstrated to be much lower than previously expected[12], likely leading to net decreases in suitable habitat at continental scales in the coming decades[13].

Relative to malaria, comparatively less is known about the net impact of climate change on *Aedes*-borne diseases. At a minimum, the distribution of *Aedes* mosquitoes is projected to shift in the face of climate change, with a mix of expansions in some regions and contractions in others, and no overwhelming net global pattern of gains or losses[3,8]. The consequences of those range shifts for disease burden are therefore likely to be important, but can be challenging to summarize across landscapes and pathogens. Of all *Aedes*-borne diseases, dengue fever has been most frequently modeled in the context of climate change, and several models of the potential future of dengue have been published over the last two decades, with limited work building consensus among them[4]. Models relating temperature to vectorial capacity, and applying general circulation models (GCMs) to predict the impacts of climate change, go back as far as the late 1990s[5]. A study from 2002 estimated that the population at risk (PAR) from dengue would rise from 1.5 billion in 1990, to 5-6 billion by 2085, as a result of climate change[14]. A more recent study suggested that climate change alone should increase the global dengue PAR by 0.28 billion by 2050, but accounting for projected changes in global economic development (using GDP as a predictor for dengue risk) surprisingly reduces the projected PAR by 0.12 billion over the same interval[15]. Mechanistic models have shown that increases or decreases in dengue risk can be predicted for the same region based on climate models, scenario selection, and regional variability[16].

Chikungunya and Zika viruses, which have emerged more recently as a public health crisis, are less well-studied in the context of climate change. A monthly model for chikungunya in Europe, constrained by the presence of *Ae. albopictus*, found that the A1B and B1 scenarios both correspond to substantial increases in chikunguya risk surrounding the Mediterranean[17]. A similar modeling study found that dengue is likely to expand far more significantly due to climate change than Zika[9] (though epidemiological differences among these three viruses remain unresolved[18–20]). However, the combined role of climate change and El Niño has already been suggested as a possible driver of the 2016 Zika pandemic's severity[9]. Global mechanistic forecasts accounting for climate change are all but nonexistent

for both diseases, given how recently both emerged as public health crises, and how much critical information is still lacking in the basic biology and epidemiology of both pathogens.

In this study, we apply a new mechanistic model of the spatiotemporal distribution of *Aedes*-borne viral outbreaks, to resolve the role climate change could play in global transmission of dengue, chikungunya, and Zika. Whereas other mechanistic approaches rely on methods like dynamic energy budgets to build complex biophysical models for *Aedes* mosquitoes[21,22], and subsequently (sometimes) extrapolate potential epidemiological dynamics[5], our approach uses a single basic cutoff for the thermal interval where viral transmission is possible. The simplicity and transparency of the method masks a sophisticated underlying model that links the basic rate of reproduction R_0 for *Aedes*-borne viruses to temperature, via experimentally-determined physiological response curves for traits like biting rate, fecundity, mosquito lifespan, extrinsic incubation rate, and transmission probability. The model is easily projected into geographic space by defining model based measures of suitability and classifying each location in space as suitable or not. We take a Bayesian approach in order to take into account uncertainty in the experimental data. We determine our suitability thresholds for transmission by calculating the temperature values at which the posterior probability that $R_0 > 0$ exceeds 97.5%. For *Aedes aegypti*, these bounds are 21.3—34.0 C, and for *Aedes albopictus*, 19.9—29.4 C. This threshold condition defines the temperatures at which transmission is not prevented, rather than the more familiar threshold at which disease invasion is expected ($R_0 > 1$, which cannot be predicted in the absence of additional information on vector and human population sizes and other factors). We then classify each location by suitability in each month based on already published projections for current climates in the Americas[6]. Here, we expand the framework for both *Ae. aegypti* and *Ae. albopictus* to project cumulative months of suitability in current and future (2050 and 2070) climates, and further examine how global populations at risk might change in different climate change scenarios. In doing so, we provide the first mechanistic forecast for the potential future transmission risk of chikungunya and Zika, which have been forecasted primarily via phenomenological methods (like ecological niche modeling[9]). Our study is also the first to address the seasonal aspects of population at risk for *Aedes*-borne diseases in a changing climate.

We found that the current pattern of suitability suggested by our model based on mean monthly temperatures (**Figure 1**) reproduces the known or projected distributions of dengue[23], chikungunya[24], and Zika[9,25,26] well. For both *Ae. aegypti* and *Ae. albopictus*, most of the tropics is currently optimal for viral transmission year-round, with suitability declining along latitudinal gradients. Many temperate regions are suitable for up to 6 months of the year currently, but outside the areas mapped as "suitable" by disease-specific distribution models; in some cases, limited outbreaks may only happen when cases are imported from travelers (e.g. in northern Australia, where dengue is not presently endemic but outbreaks happen in suitable regions[16]; or in mid-latitude regions of the United States, where it has been suggested that traveler cases could result in limited autochthonous transmission[25,27]). Transmission models in current climates, and derived maps of seasonal population at risk, were extremely sensitive to whether minimum, mean, or maximum monthly temperatures were used (**Figure S1-4**). Under current climates, maximum temperatures predict a consistently worse pattern of population-at-risk (PAR) from *Ae. aegypti* than minimum temperatures. For *Ae. albopictus*, the pattern is less straightforward, with maximum temperatures predicting the worst outcome (highest number of people at risk) for shorter periods, but with minimum temperatures producing a worse pattern of risk measured by 6 or more months of suitability (**Figure 2**). Perhaps most compelling, transmission curves generated by mean temperatures do not align neatly with either maximum or minimum curve, potentially demonstrating a downside of disease forecasts that do not account for the extreme ends of normal temperature variation. Resolving uncertainty in future climate-based disease forecasts requires resolving how temperature regimes as a whole (encapsulated by minimum, mean, and maximum monthly temperatures) translate into transmission potential.

The most surprising result of our study is that the upper thermal bound of *Aedes* viral transmission is likely to be increasingly relevant in a changing climate—even in localities with current year-round transmission. For *Ae. aegypti*, minimum temperatures produce far lower total extents of transmission, though the extent of year-round transmission is roughly comparable; the pattern is reversed for *Ae. albopictus*, for which the cumulative extent is the same, but minimum monthly temperatures predict year-round transmission risk for 1-2 billion more people (**Figure 2**). This is ultimately an

emergent property of the same seasonal risk curves generated for current temperatures, and has key implications for interpreting the climate-disease relationship. (In particular, partial mitigation of climate change could keep *Ae. albopictus* mosquitoes especially within optimal thermal ranges for more of the year, and thereby produce worse clinical outcomes). Furthermore, for both mosquitoes, inter-annual and intra-monthly variation in weather may also have a more significant effect on viral outbreak outcomes than subtler variations in overall climate trends. Increasing climate change severity increases population at risk for both mosquitoes when using minimum temperatures but decreases it for *Ae. albopictus* transmission, using maximum temperatures (**Figure 3**). Moreover, the range of temperatures forecasted for a given month across scenarios produce a more dramatic range of risk forecasts than any combination of climate models and pathways.

In the face of a changing climate, dramatic changes can be expected in the global spatiotemporal risk patterns from both *Ae. aegypti* (**Figure 4**) and *Ae. albopictus* (**Figure 5**). For minimum monthly temperatures, models for both mosquitoes in 2050 under the most and least optimistic pathways (RCPs 2.6 and 8.5) are quite different from current distributions, with the most notable changes being a southward shift of year-round suitable area in sub-Saharan Africa, an increase in months of suitability over a larger area in the Americas, an increase in suitable area through southern Europe, and an expansion of the northern range limits of transmission for both Europe and North America. In contrast, for maximum temperature scenarios for 2050, much more idiosyncratic distributional patterns develop. Both mosquitoes gain significant ground towards the poles for at least a few months of the year. In some cases, climate change is expected to reverse well-documented geographic patterns of transmission, like Australia's latitudinal gradient (with current transmission risk highest on the northern coast, but projected to shift towards the southern and eastern coasts by 2050). While some core areas (like the Amazon or Indian subcontinent) become less suitable for year round transmission for *Ae. aegypti*, the overall pattern is one of expanding thermally-suitable area in sub-Saharan Africa, Central America, and the Andes. Whether this translates into increased vector establishment will depend heavily on land use patterns and urbanization at regional scales, a fact that may ultimately buffer some regions like the Andes from

increased disease risk[28,29]. In contrast, for *Ae. albopictus*, future risk patterns change far more dramatically, primarily because maximum temperature scenarios produce large reductions in range (**Figure 5**), corresponding to 1-2 billion fewer people at risk of year-round transmission even though the overall extent of suitability is roughly the same with minima and maxima (**Figure 2**). In the most extreme warming scenarios, the tropics become unsuitable year-round, with the only projected year-round transmission projected for high-elevation regions like the Andes mountains, or isolated patches of Africa and southeast Asia (**Figure 5**).

Our model predicts that 6.1 billion people currently live in areas suitable for *Ae. aegypti* transmission at least part of the year (i.e., 1 month or more) and 6.49 billion in areas suitable for *Ae. albopictus* transmission (using mean temperatures). Whether future risk will be driven by rising minimum temperatures, moving people into suitable transmission temperatures, or instead maximum temperatures curbing transmission, as people are exposed to temperatures above suitable ranges, remains to be seen. However, we can anticipate each of these, using our modeling approaches, and see that they give us quite different predictions. Based on comparisons of predicted monthly minimum and maximum temperatures (min/max) instead of means, current people at risk (PAR) in areas suitable for *Ae. Aegypti* based transmission are 4.30/7.15 billion and for *Ae. albopictus* are 4.82/6.49 billion. An average (across RCPs and GCMs) of 5.12/7.24 billion people live in areas facing increased exposure to climate suitability for *Ae. aegypti*-borne viruses by 2050 (5.33/7.21 billion by 2070), while 5.57/5.82 billion live in areas facing increased exposure to climate suitability for *Ae. albopictus*-borne viruses by 2050 (5.77/5.61 billion by 2070). It is important to note that these changes represent shifts in location of suitable climates, so new individuals will become exposed, while others will see decreasing risk. A total of 85,118/2,881,487,129 people live in areas likely to experience *decreased* climate suitability for exposure to transmission by *Ae. aegypti* by 2050 (585,895/3,394,798,283 by 2070), and an even more surprising 234,623,576/3,895,574,225 face decreased climate suitability for exposure to transmission by *Ae. albopictus* by 2050 (387,799,583/4,243,005,789 by 2070). Interestingly, 21,233/69,986,579 people live in areas predicted to entirely escape viral transmission by *Ae. aegypti*, and 28,277/922,980,947 are likely to

escape *Ae. albopictus* transmission, by 2070. These decreases suggest that climate change may not cause a direct global spike in *Aedes*-borne disease, and could ultimately mitigate it; however, gains in exposure may have a more visible effect than losses on realized disease outcomes, given the potential for explosive outbreaks (like Zika in the Americas) when viruses are first introduced into naïve populations[30]. The emergence of a Zika pandemic in the Old World, of chikungunya in Europe[17], or of dengue anywhere the virus (or any given serotype) is not endemic, is still a critical concern. Whereas the highest risk is consistently obvious in south and southeast Asia, the most significant hotspots of *uncertainty* in our seasonal population at risk maps is evident in Europe and sub-Saharan Africa (**Figure S5, S6**), and we suggest that these especially require further, locally-tailored investigation by public health researchers.

While climate change poses perhaps the most serious growing threat to global health security, the relationship between climate change and worsening clinical outcomes for *Aedes*-borne diseases is unlikely to be straightforward. In practice, shifting patterns of suitability will correspond to different local patterns of exposure in a changing climate, independent of broader geographic constraints. The link from transmission risk to clinical outcomes is confounded by other health impacts of climate change, including changing precipitation patterns, socioeconomic development, changing patterns of land use and urbanization, potential vector (and virus) evolution and adaptation to warming temperatures, and changing healthcare landscapes, all of which covary strongly (potentially leading to complex nonlinearities). Together these will determine the burden of *Aedes*-borne outbreaks. Moreover, human adaptation to climate change will matter just as much as mitigation in determining how risk patterns shift; for example, increased drought stress will likely correspond to water storage that increases proximity to *Aedes* breeding habitat[31]. Our models only provide an outer spatiotemporal bound to where transmission of dengue, chikungunya, and Zika is thermally plausible; climate change is likely to change the risk-burden relationship at fine scales within those zones of transmission in nonlinear ways, such that areas with shorter seasons of transmission could still experience worse overall disease burdens, or vice versa. As *Aedes*-borne diseases shift, research building consensus between our models and others, that works towards refine risk assessments within experimentally-determined outer bounds is paramount[32].

Methods

The Bayesian Model

Our study presents geographic projections of a published experimentally-derived mechanistic model of *Aedes* viral transmission. The approach to fit the thermal responses in a Bayesian framework and combine them to obtain the posterior distribution of R_0 as a function of these traits is described in detail in Johnson *et al.*[7] and the particular traits and fits for *Aedes aegypti* and *Ae. albopictus* are presented in Mordecai *et al.*[33]. Once we obtain our posterior samples for R_0 as a function of temperature we can evaluate the probability that $R_0 > 0$ (Prob($R_0 > 0$)) at each temperature, giving a distinct curve for each mosquito species. We then define cutoff of Prob($R_0 > 0$) = α to determine our estimates of the thermal niche. For all except Figure 2 we use $\alpha = 0.975$. This very high probability allows us to isolate a temperature window for which transmission is almost certainly not excluded. For Figure 2, points correspond to $\alpha = 0.5$ and the lower/upper error bars to $\alpha = 0.975$ and 0.025 respectively. Note that the smaller probability leads to larger population at risk estimates because the lower cutoff results in a wider thermal niche (i.e., temperatures where there is even a small chance that transmission could be permitted).

Current & Future Climates

Current mean, maximum, and minimum monthly temperature data was derived from the WorldClim dataset (www.worldclim.org).[34] For future climates, we selected general circulation models (GCMs) that are most commonly used by studies forecasting species distributional shifts, at a set of four representative concentration pathways (RCPs) that account for different global responses to mitigate climate change. These are the Beijing Climate Center Climate System Model (BCC-CSM1.1); the Hadley GCM (HadGEM2-CC and HadGEM2-ES); and the National Center for Atmospheric Research's Community Climate System Model (CCSM4). Each of these can respectively be forecasted for RCP 2.6, RCP 4.5, RCP 6.0 and RCP 8.5. RCP numbers correspond to increased radiation in W/m^2 by the year 2100,

therefore expressing scenarios of increasing severity. (However, even these scenarios are nonlinear over time. For example, in 2050, RCP 4.5 is a more severe change than 6.0; see **Figure 3.**) For future climate scenarios, only minimum and monthly maximum projected temperatures are available. For most visualizations presented in the main paper (Figures 3 & 4), we used the HadGEM2-ES model, the most commonly used GCM. The mechanistic transmission model was projected onto the climate data using the 'raster' package in R 3.1.1. Subsequent visualizations were generated in ArcMap.

Population at Risk

To quantify a measure of risk, comparable between current and future climate scenarios, we used population count data from the Gridded Population of the World, version 4 (GPW4)[35], predicted for the year 2015. We selected this particular population product as it is minimally modeled *a priori*, ensuring that the distribution of population on the earth's surface has not been predicted by modeled covariates that would also influence our mechanistic vector-borne disease model predictions. These data are derived from most recent census data, globally, at the smallest administrative unit available, then extrapolated to produce continuous surface models for the globe for 5-year intervals from 2000-2020. These are then rendered as globally gridded data at 30 arc-seconds; we aggregated these in R (raster[30]) to match the climate scenario grids at 5 minute resolution (approximately $10km^2$ at the equator). We used 2015 population count as our proxy for current, and explored future risk relative to the current population counts. This prevents arbitrary demographic model-imposed patterns emerging, possibly obscuring climate generated change. We note that these count data reflect the disparities in urban and rural patterns appropriately for this type of analysis, highlighting population dense parts of the globe. Increasing urbanization would likely amplify the patterns we see, as populations increase overall, and the lack of appropriate population projections at this scale for 30-50 years in the future obviously limits the precision of the forecasts we provide.

Acknowledgements

This work was funded by the National Science Foundation (DEB-1518681 to SJR, LRJ, EAM,NSF DEB-1641145 to SJR, and DEB-1640780 to EAM), the Stanford Woods Institute for the Environment (https://woods.stanford.edu/research/environmental- venture-projects), and the Stanford Center for Innovation in Global Health (http://globalhealth. stanford.edu/research/seed-grants.html). Van Savage, Naveed Heydari, Jason Rohr, Matthew Thomas, and Marta Shocket provided helpful discussions on modeling approaches.

Author Information

The authors declare no competing interests. Correspondence and requests for materials should be addressed to S.J.R. (sjryan@ufl.edu).

Author Contributions

SJR initiated the idea for the study. SJR and LJ ran the models. CJC, SJR, EAM, and LJ wrote the manuscript. SJR and CJC made the figures.

References

1. Hoberg, E. P. & Brooks, D. R. Evolution in action: climate change, biodiversity dynamics and emerging infectious disease. *Phil Trans R Soc B* **370,** 20130553 (2015).
2. Lafferty, K. D. The ecology of climate change and infectious diseases. *Ecology* **90,** 888–900 (2009).
3. Escobar, L. E. *et al.* Declining Prevalence of Disease Vectors Under Climate Change. *Sci. Rep.* **6,** (2016).
4. Messina, J. P. *et al.* The many projected futures of dengue. *Nat. Rev. Microbiol.* **13,** 230–239 (2015).
5. Patz, J. A., Martens, W., Focks, D. A. & Jetten, T. H. Dengue fever epidemic potential as projected by general circulation models of global climate change. *Environ. Health Perspect.* **106,** 147 (1998).
6. Mordecai, E. *et al.* Detecting the impact of temperature on transmission of Zika, dengue, and chikungunya using mechanistic models. *PLoS Negl. Trop. Dis.* **11,** e0005568 (2017).
7. Johnson, L. R. *et al.* Understanding uncertainty in temperature effects on vector-borne disease: a Bayesian approach. *Ecology* **96,** 203–213 (2015).
8. Campbell, L. P. *et al.* Climate change influences on global distributions of dengue and chikungunya virus vectors. *Phil Trans R Soc B* **370,** 20140135 (2015).
9. Carlson, C. J., Dougherty, E. R. & Getz, W. An ecological assessment of the pandemic threat of Zika virus. *PLoS Negl Trop Dis* **10,** e0004968 (2016).
10. Githeko, A. K., Lindsay, S. W., Confalonieri, U. E. & Patz, J. A. Climate change and vector-borne diseases: a regional analysis. *Bull. World Health Organ.* **78,** 1136–1147 (2000).
11. Ibelings, B. *et al.* Chytrid infections and diatom spring blooms: paradoxical effects of climate warming on fungal epidemics in lakes. *Freshw. Biol.* **56,** 754–766 (2011).
12. Mordecai, E. A. *et al.* Optimal temperature for malaria transmission is dramatically lower than previously predicted. *Ecol. Lett.* **16,** 22–30 (2013).
13. Ryan, S. J. *et al.* Mapping physiological suitability limits for malaria in Africa under climate change. *Vector-Borne Zoonotic Dis.* **15,** 718–725 (2015).

14. Hales, S., De Wet, N., Maindonald, J. & Woodward, A. Potential effect of population and climate changes on global distribution of dengue fever: an empirical model. *The Lancet* **360,** 830–834 (2002).

15. \AAström, C. *et al.* Potential distribution of dengue fever under scenarios of climate change and economic development. *Ecohealth* **9,** 448–454 (2012).

16. Williams, C. *et al.* Projections of increased and decreased dengue incidence under climate change. *Epidemiol. Infect.* 1–10 (2016).

17. Fischer, D. *et al.* Climate change effects on Chikungunya transmission in Europe: geospatial analysis of vector's climatic suitability and virus' temperature requirements. *Int. J. Health Geogr.* **12,** 51 (2013).

18. Funk, S. *et al.* Comparative analysis of dengue and Zika outbreaks reveals differences by setting and virus. *PLoS Negl. Trop. Dis.* **10,** e0005173 (2016).

19. Bastos, L. *et al.* Zika in Rio de Janeiro: assessment of basic reproductive number and its comparison with dengue. *BioRxiv* 055475 (2016).

20. Riou, J., Poletto, C. & Boëlle, P.-Y. A comparative analysis of Chikungunya and Zika transmission. *Epidemics* (2017).

21. Kearney, M., Porter, W. P., Williams, C., Ritchie, S. & Hoffmann, A. A. Integrating biophysical models and evolutionary theory to predict climatic impacts on species' ranges: the dengue mosquito Aedes aegypti in Australia. *Funct. Ecol.* **23,** 528–538 (2009).

22. Hopp, M. J. & Foley, J. A. Global-scale relationships between climate and the dengue fever vector, Aedes aegypti. *Clim. Change* **48,** 441–463 (2001).

23. Bhatt, S. *et al.* The global distribution and burden of dengue. *Nature* **496,** 504–507 (2013).

24. Nsoesie, E. O. *et al.* Global distribution and environmental suitability for chikungunya virus, 1952 to 2015. *Euro Surveill. Bull. Eur. Sur Mal. Transm. Eur. Commun. Dis. Bull.* **21,** (2016).

25. Samy, A. M., Thomas, S. M., Wahed, A. A. E., Cohoon, K. P. & Peterson, A. T. Mapping the global geographic potential of Zika virus spread. *Mem. Inst. Oswaldo Cruz* **111,** 559–560 (2016).

26. Messina, J. P. *et al.* Mapping global environmental suitability for Zika virus. *Elife* **5,** e15272 (2016).

27. Bogoch, I. I. *et al.* Anticipating the international spread of Zika virus from Brazil. *Lancet Lond. Engl.* **387,** 335–336 (2016).

28. Grau, H. R. *et al.* The ecological consequences of socioeconomic and land-use changes in postagriculture Puerto Rico. *AIBS Bull.* **53,** 1159–1168 (2003).

29. Li, Y. *et al.* Urbanization increases Aedes albopictus larval habitats and accelerates mosquito development and survivorship. *PLoS Negl. Trop. Dis.* **8,** e3301 (2014).

30. Lucey, D. R. & Gostin, L. O. The emerging Zika pandemic: enhancing preparedness. *Jama* **315,** 865–866 (2016).

31. Beebe, N. W., Cooper, R. D., Mottram, P. & Sweeney, A. W. Australia's dengue risk driven by human adaptation to climate change. *PLoS Negl. Trop. Dis.* **3,** e429 (2009).

32. Carlson, C. J., Dougherty, E., Boots, M., Getz, W. & Ryan, S. Consensus and conflict among ecological forecasts of Zika virus outbreaks in the United States. *bioRxiv* 138396 (2017).

33. Mordecai, E. A. *et al.* Detecting the impact of temperature on transmission of Zika, dengue, and chikungunya using mechanistic models. *PLoS Negl. Trop. Dis.* **11,** e0005568 (2017).

34. Hijmans, R. J., Cameron, S. E., Parra, J. L., Jones, P. G. & Jarvis, A. Very high resolution interpolated climate surfaces for global land areas. *Int. J. Climatol.* **25,** 1965–1978 (2005).

35. Center for International Earth Science Information Network (CIESIN), Columbia University. *Gridded Population of the World, Version 4 (GPWv4).* (US NASA Socioeconomic Data and Applications Center (SEDAC), 2016).

36. Hijmans, R. J. & van Etten, J. *raster: Geographic analysis and modeling with raster data.* (2012).

342 **Figures**

343 **Figure 1 | Mapping current transmission risk.** Maps of current monthly suitability based on mean

344 temperatures for a temperature suitability threshold corresponding to the posterior probability that scaled

345 $R_0 > 0$ is 97.5% for (a) *Aedes aegypti* and (b) *Aedes albopictus.*

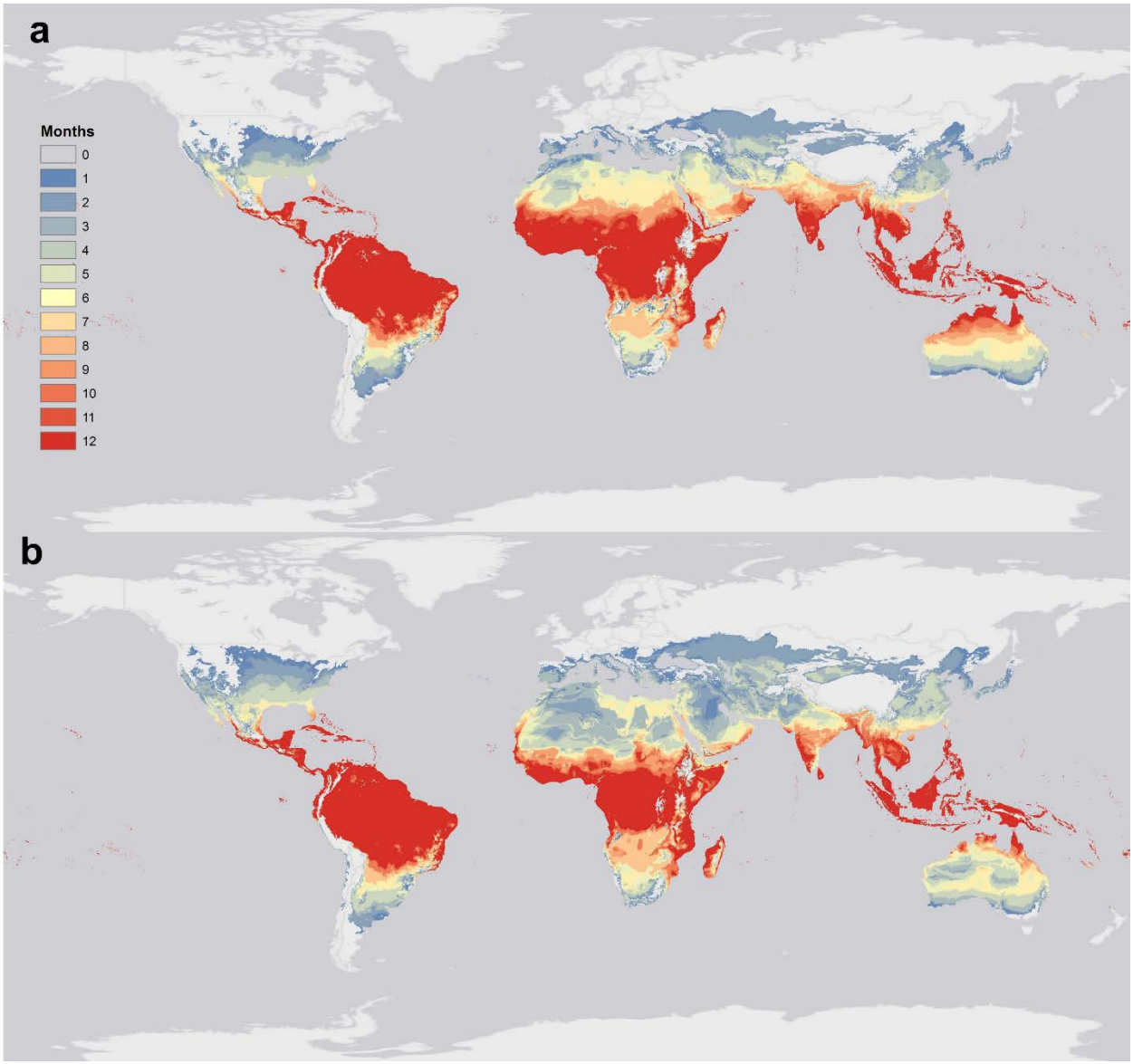

346

347

348

349

350

Figure 2 | Current and future global population-at-risk. Values correspond to population at risk for a given minimum number of months. Points correspond to the 50% posterior probability that scaled $R_0 > 0$, while confidence intervals correspond to probabilities of 2.5% and 97.5%. Left and right: *Aedes aegypti* and *Aedes albopictus*. Current models are separated by mosquito and by monthly minimum, mean, or maximum temperature; future model colors also reflect representative concentration pathways (RCPs) and minimum vs. maximum monthly temperature (see legend), while contrasting GCMs are plotted as separate trajectories with the same plotting scheme.

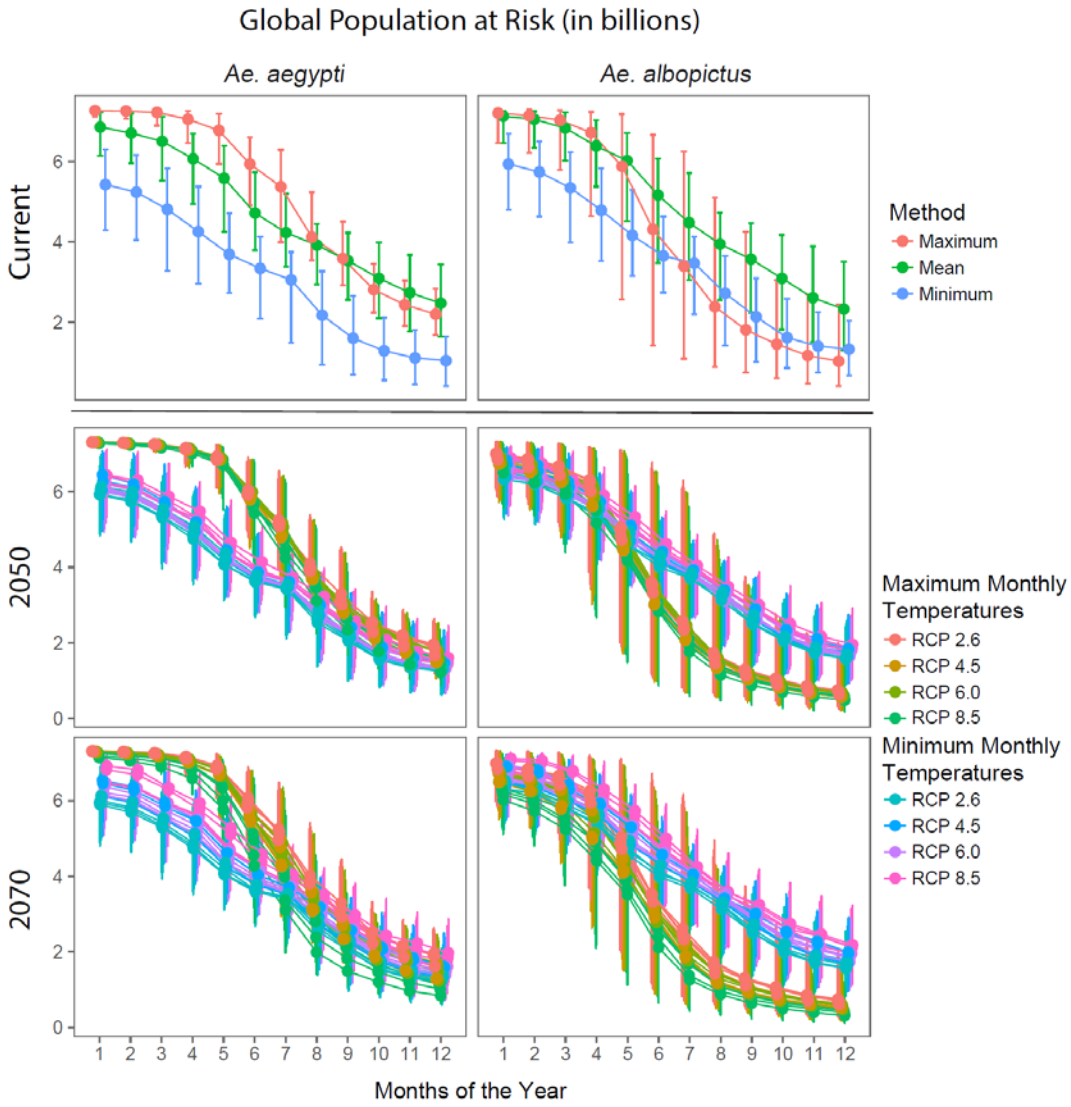

361 **Figure 3 |** Projected total changes in global population at risk (PAR, for one or more months), for *Aedes*
362 *aegypti* and *Aedes albopictus* transmission, from current modeled PAR, as a function of minimum (T_{min})
363 and maximum (T_{max}) monthly temperatures, to 2050 and 2070, by representative climate pathways
364 (RCPs), across 4 general circulation models.

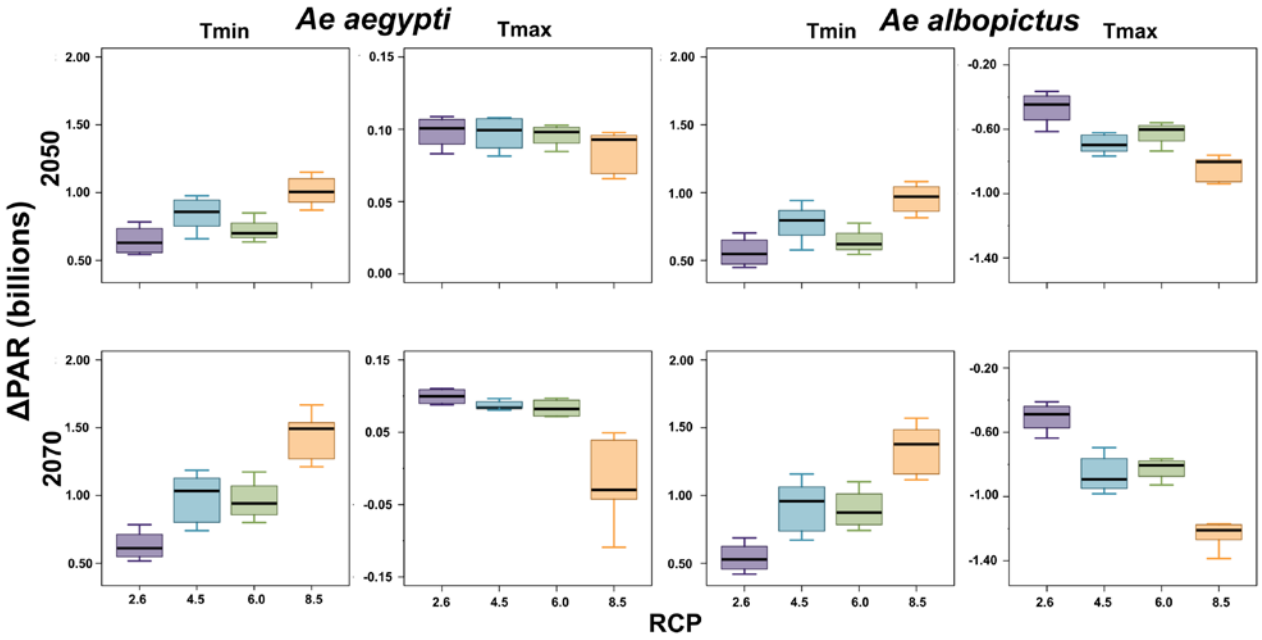

365

366 **Figure 4 | Mapping future transmission risk scenarios for *Aedes aegypti*.** Maps of monthly suitability
367 based on a temperature threshold corresponding to the posterior probability that scaled $R_0 > 0$ is greater or
368 equal to 97.5%, for transmission by *Aedes aegypti* for predicted minimum (T_{min}, Left - a,c,e) and
369 maximum (T_{max}, Right - b,d,f) monthly temperatures under current (a,b) and future scenarios (HadGEM2-
370 ES 2050 for RCP 2.6 (c,d) and RCP 8.5 (e,f).

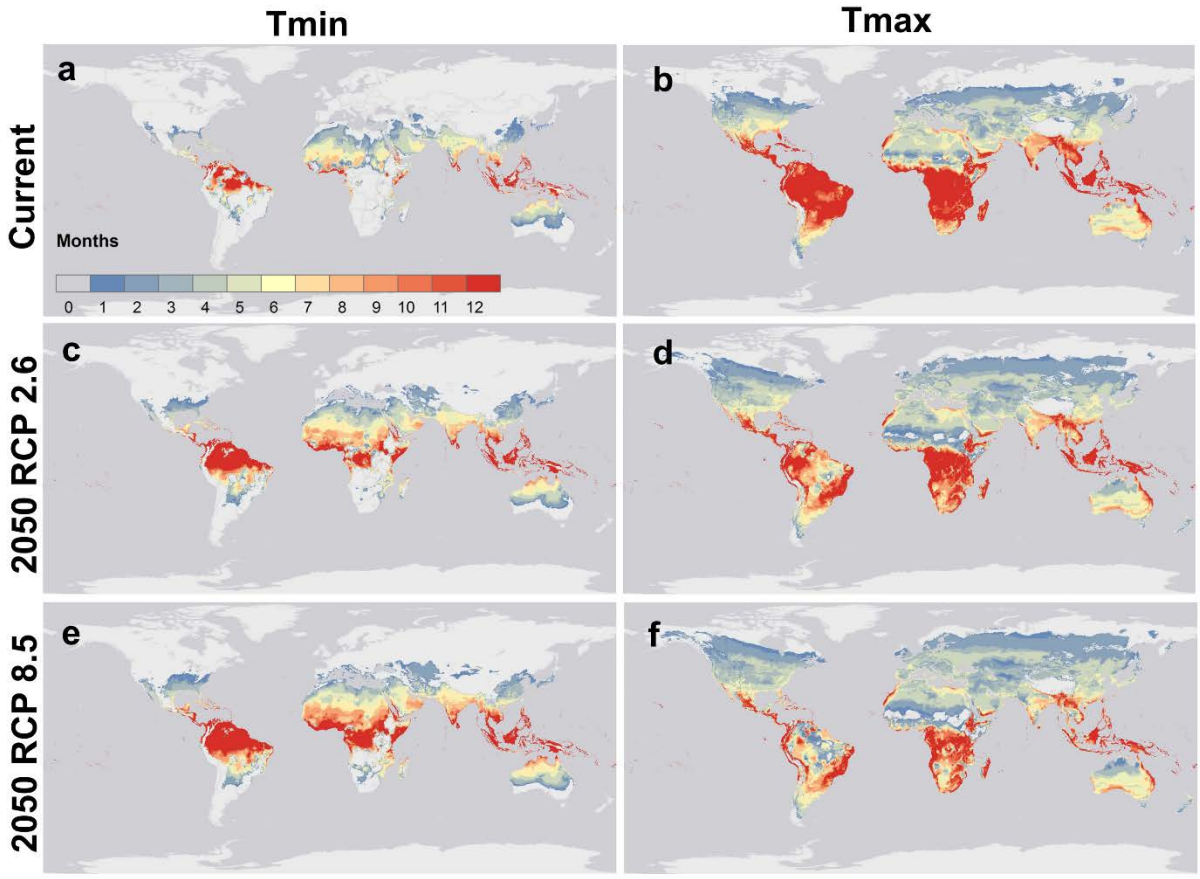

371

372

373 **Figure 5 | Mapping future transmission risk scenarios for *Aedes albopictus.*** Maps of monthly
374 suitability based on a temperature threshold corresponding to the posterior probability that scaled $R_0 > 0$ is
375 greater or equal to 97.5%, for transmission by *Aedes albopictus* for predicted minimum (T_{min}, Left - a,c,e)
376 and maximum (T_{max}, Right - b,d,f) monthly temperatures under current (a,b) and future scenarios
377 (HadGEM2-ES 2050 for RCP 2.6 (c,d) and RCP 8.5 (e,f).

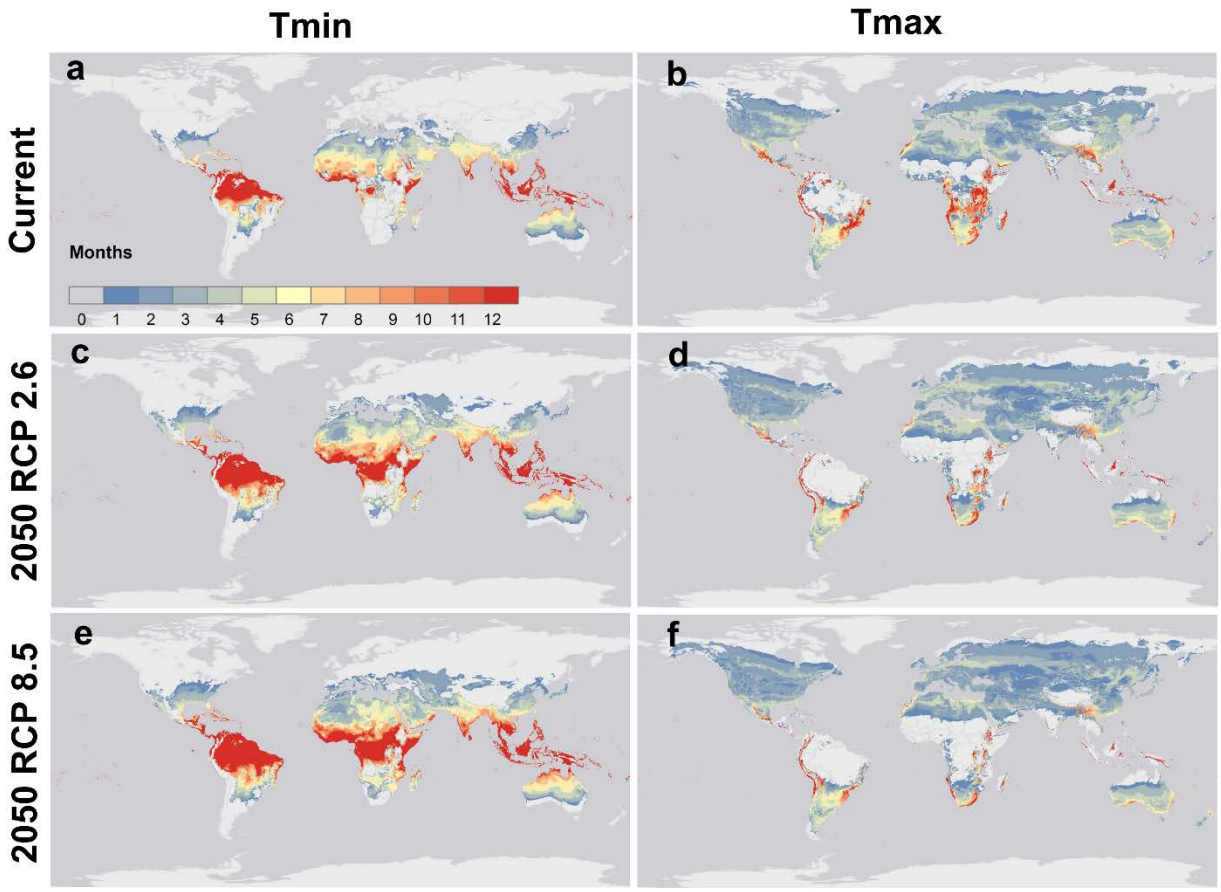

378

379

380 **Figure S1 |** Current months of the year suitable for *Ae aegypti* transmission for (a) minimum, (b) mean,

381 and (c) maximum monthly temperatures, where the posterior probability that scaled $R_0 > 0$ is greater or

382 equal to 97.5%.

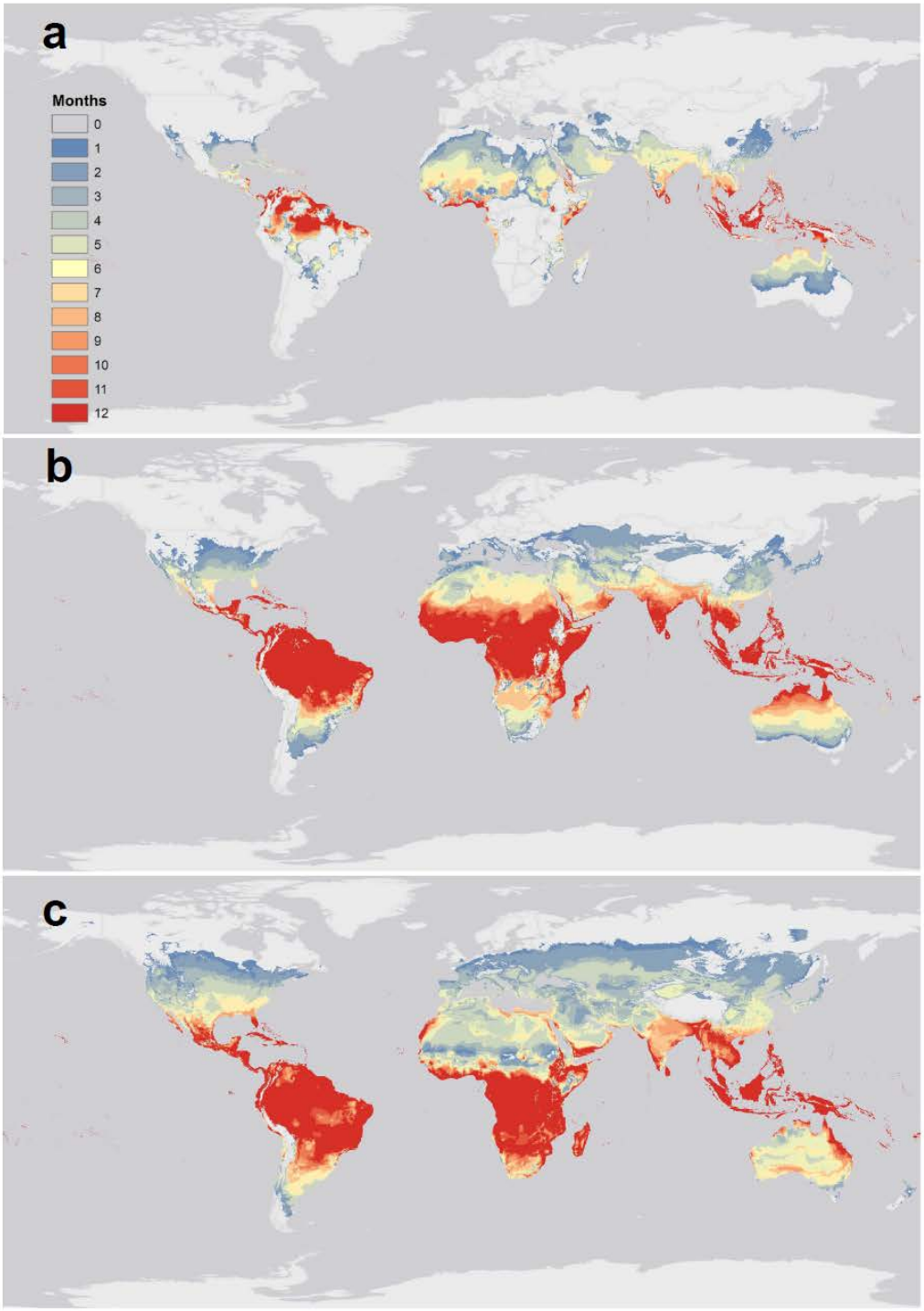

383

384 **Figure S2** | Current months of the year suitable for *Ae albopictus* transmission for (a) minimum, (b)

385 mean, and (c) maximum monthly temperatures, where the posterior probability that scaled $R_0 > 0$ is

386 greater or equal to 97.5%.

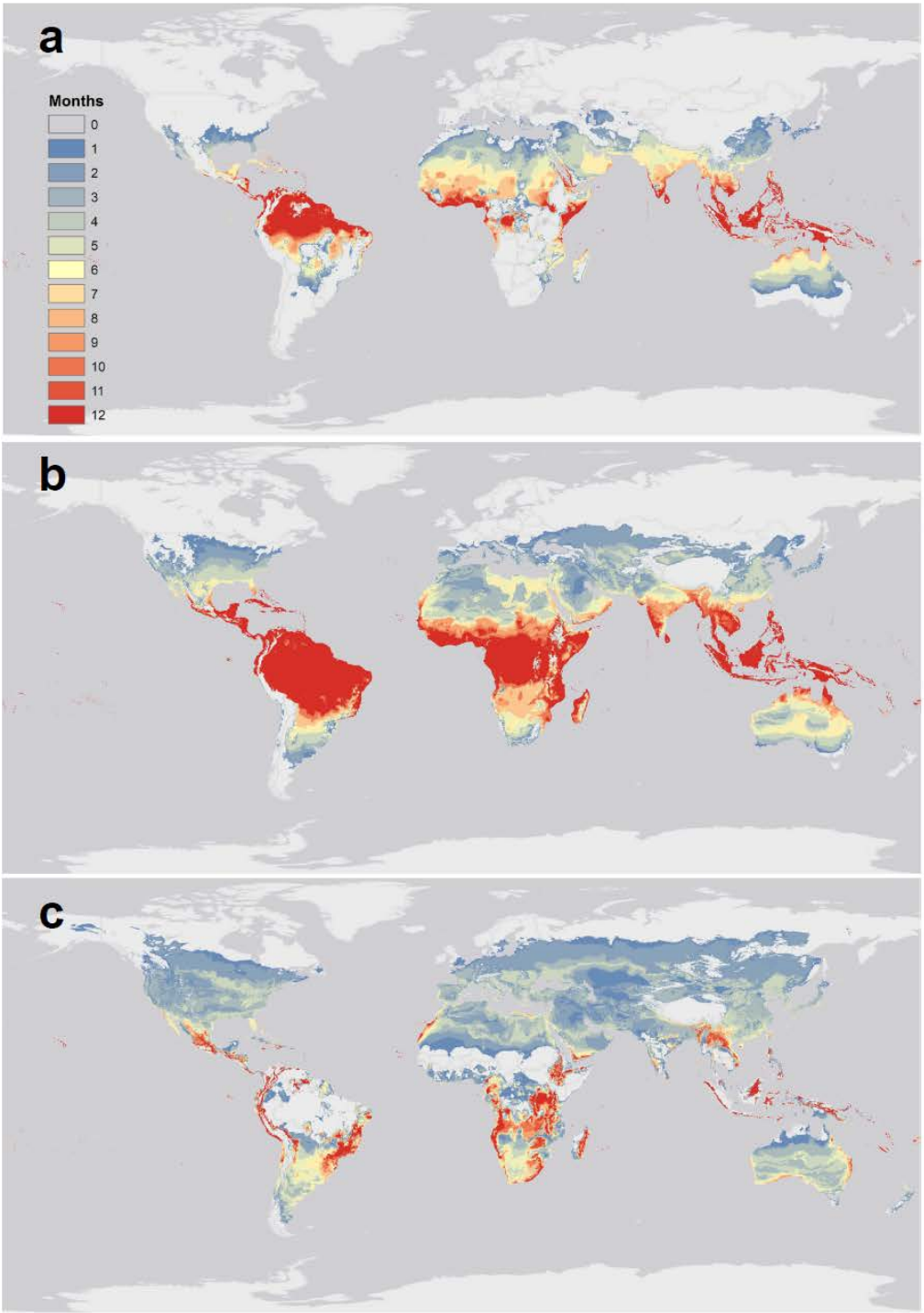

387

388 **Figure S3 |** *Aedes aegypti* current mPAR (months*people at risk), for (a) minimum, (b) mean, and (c)
389 maximum temperature. The number of months of transmission suitability generated under current
390 temperature models were multiplied by the estimated population for 2015 (Gridded Population of the
391 World GPW4[35]).

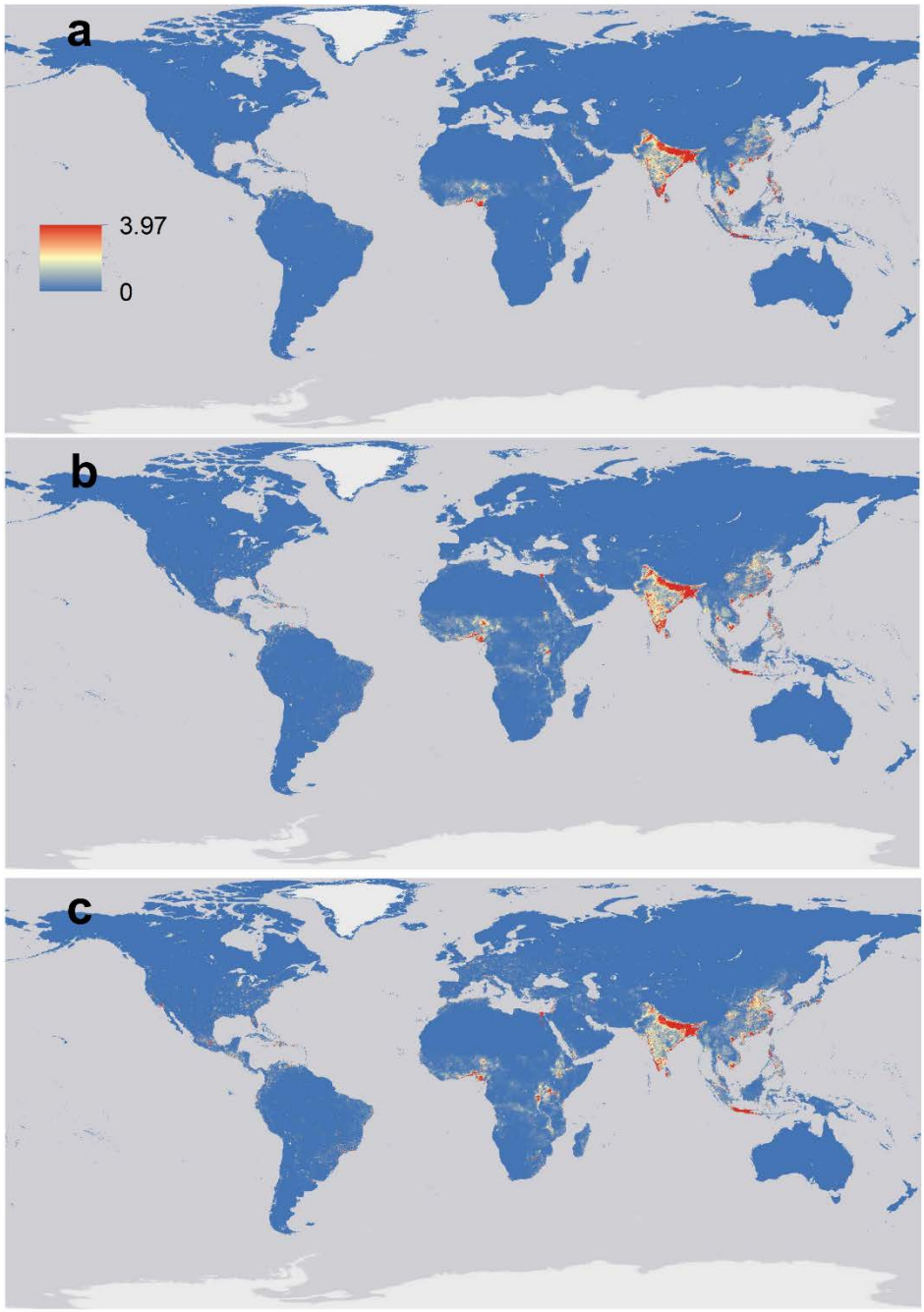

392

393 **Figure S4 |** *Aedes albopictus* current mPAR (months*people at risk), for (a) minimum, (b) mean, and (c)
394 maximum temperature. The number of months of transmission suitability generated under current
395 temperature models were multiplied by the estimated population for 2015 (Gridded Population of the
396 World GPW4[35]).

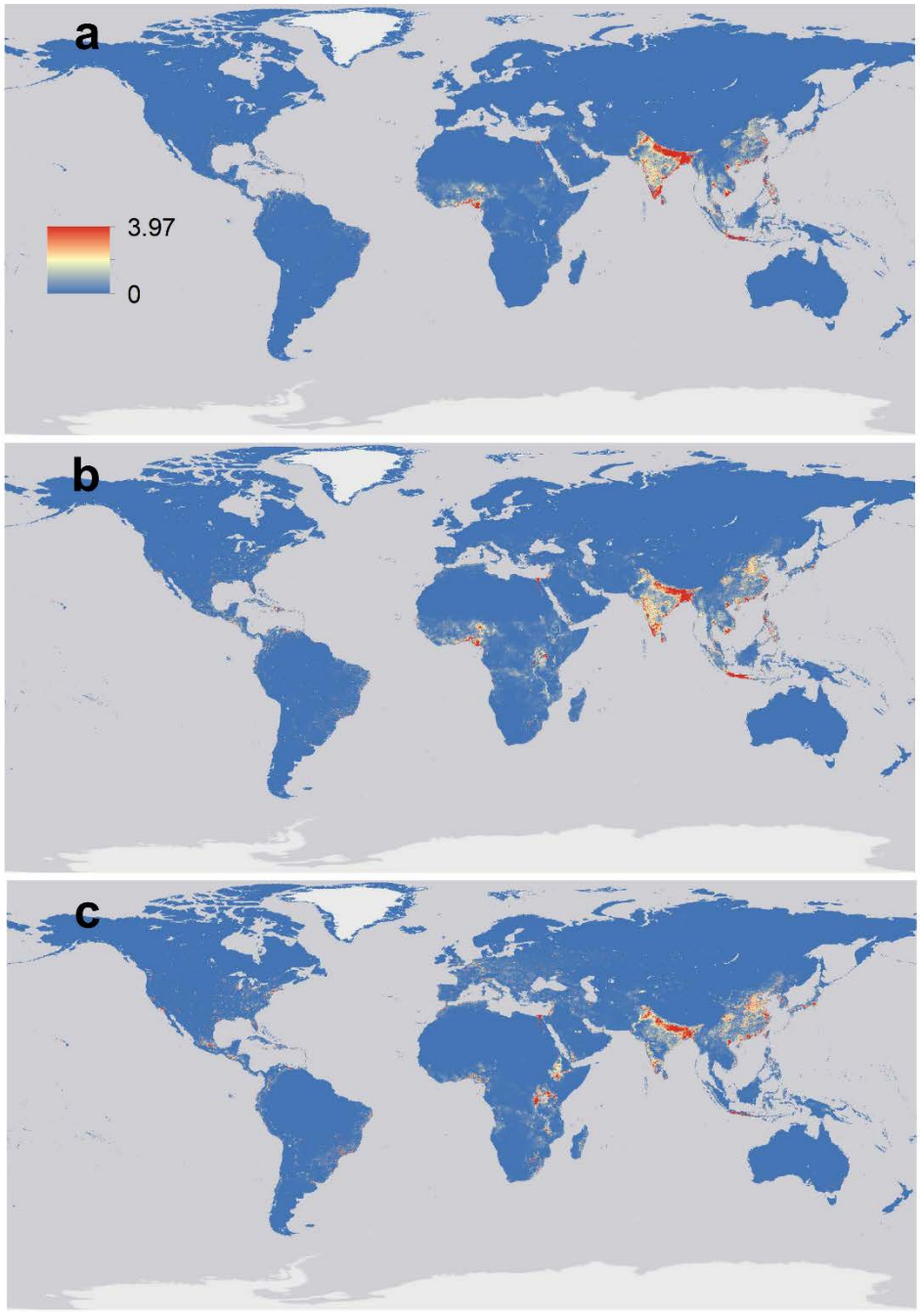

397

398

399 **Figure S5 |** *Aedes aegypti* future mPAR (months*people at risk), for (a) 2050 and (c) 2070 (max

400 HadGEM2-ES RCP 8.5), versus the highest year-round PaR for (b) 2050 and (d) 2070 (max CCSM4 RCP

401 2.6). The number of months of transmission suitability generated under temperature models were

402 multiplied by the estimated population for 2015 (Gridded Population of the World GPW4[35]).

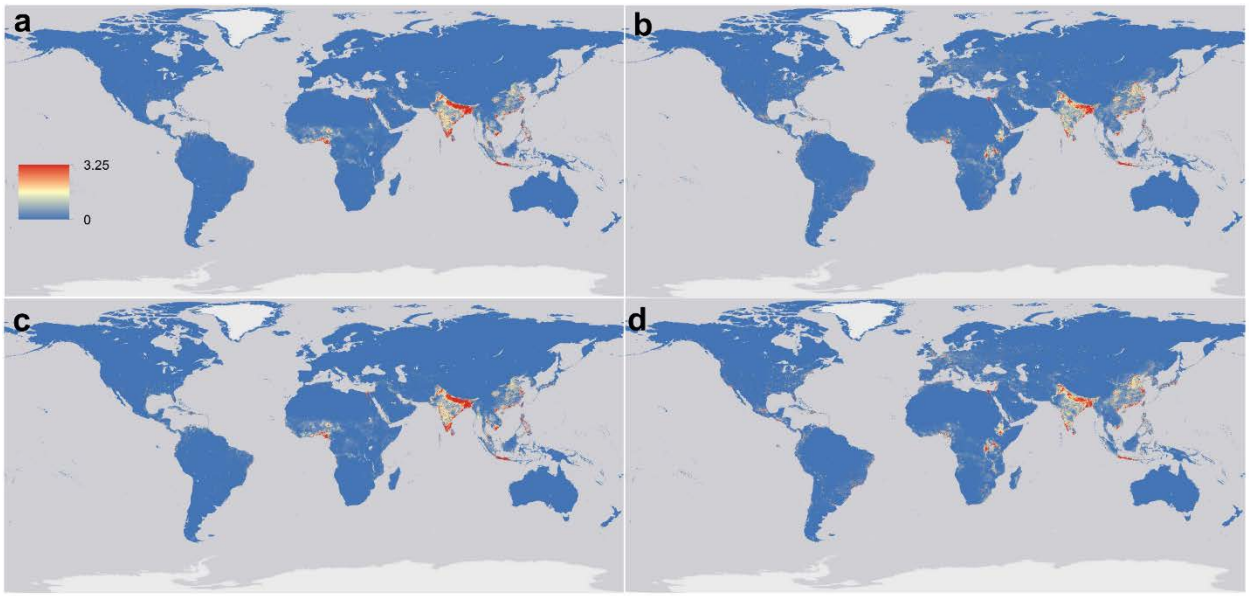

403

404

405 **Figure S6 |** *Aedes albopictus* future mPAR (months*people at risk), for (a) 2050 and (c) 2070 (max

406 HadGEM2-ES RCP 8.5), versus the highest year-round PaR for (b) 2050 and (d) 2070 (max CCSM4 RCP

407 2.6). The number of months of transmission suitability generated under temperature models were

408 multiplied by the estimated population for 2015 (Gridded Population of the World GPW4[35]).

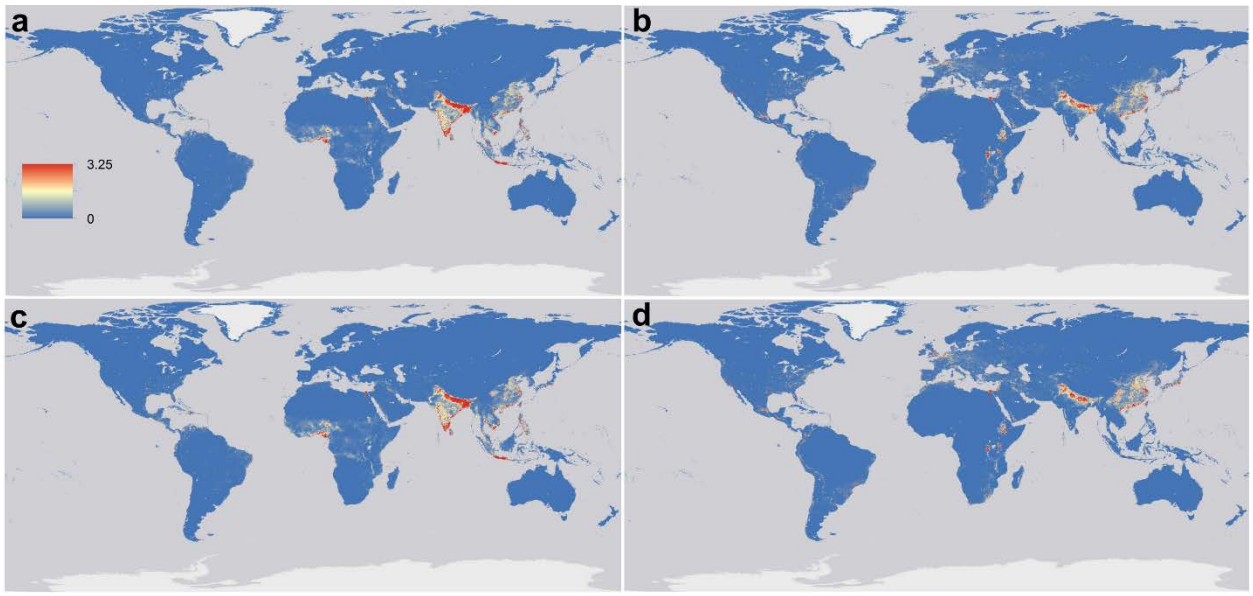

409